Building Highly Selective Hot Spots in Ag Nanoparticles Using Bifunctional Viologens: Application to the SERS Detection of PAHs

ARTICLE *in* THE JOURNAL OF PHYSICAL CHEMISTRY C · MAY 2008

Impact Factor: 4.77 · DOI: 10.1021/jp8006206 · Source: OAI

4 AUTHORS, INCLUDING:

Luca Guerrini
Medcom Advance SA
43 PUBLICATIONS **755** CITATIONS
SEE PROFILE

José Vicente García-Ramos
Spanish National Research Council
177 PUBLICATIONS **3,789** CITATIONS
SEE PROFILE

S. Sanchez-Cortes
Spanish National Research Council
197 PUBLICATIONS **4,200** CITATIONS
SEE PROFILE

THE JOURNAL OF PHYSICAL CHEMISTRY C LETTERS

2008, *112,* 7527–7530
Published on Web 04/30/2008

Building Highly Selective Hot Spots in Ag Nanoparticles Using Bifunctional Viologens: Application to the SERS Detection of PAHs

Luca Guerrini, José V. Garcia-Ramos, Concepción Domingo, and Santiago Sanchez-Cortes*

Instituto de Estructura de la Materia. CSIC. Serrano, 121, 28006-Madrid, Spain

Received: January 22, 2008; Revised Manuscript Received: March 10, 2008

The application of viologen dications in the creation of highly sensitive and selective hot spots between silver nanoparticles is reported in the present work. A method to follow the existence of such hot spots in macroscopic samples is proposed based on the plasmon absorption of these nanoparticles in suspension. The method was applied in the case of detection of the polycyclic aromatic hydrocarbon pyrene, confirming the great ability of viologens, in the increasing of the sensitivity and selectivity of the SERS technique, as both hot spot inducers and host molecules.

Surface-enhanced optical techniques are extremely sensitive analytical techniques mainly based on the giant electromagnetic (EM) enhancement induced by nanostructured noble metal surfaces and associated to their localized plasmon resonance (LPR).[1,2] During the last years, new experiments have renewed the interest in the surface-enhanced techniques, such as the possible detection of a single molecule (SMD) by surface-enhanced Raman scattering (SERS).[3,4] SMD is possible because the intensification of the EM field does not occur homogeneously on the whole metallic substrate. In fact, it is widely accepted that the main part of the electromagnetic field intensification occurs in special regions of the metallic surface called hot spots (HS).[5] Among these HS, interparticle junctions or gaps existing between metal nanoparticles (NPs) are points where the EM intensification seems to take place to a greater extent.[6] In the last year, a renewed interest in the fabrication and theoretical study of such systems can be found.[7–9] Käll et al. have studied in detail the enhancement resulting from these gaps, leading to the conclusion that the distance and the excitation wavelength play an important role.[8] It is generally accepted that the possibility of SMD depends on the existence of interparticle HS.[7] However, the fabrication of such HS escapes from the experimental control in macroconditions, being that their existence is a matter of luck provided by the specific aggregation pattern and the morphology induced by aggregates adsorbed on NPs. Thus, the molecules adsorbed on the metal surface may effectively play a crucial role in the formation of these HS.

In this sense, Moskovits et al. have recently started a series of experiment aimed to induce the formation of HS by using bifunctional thiol-containing adsorbates.[10,11] On the other hand, metal NPs in suspension seem to be the best substrate to induce a high EM intensification.[12] We propose to go further in the fabrication of HS by using molecules providing a double function, inducing the formation of HS, by virtue of their bifunctional nature and their ability to interact strongly with the surface, thus acting as molecular hosts in the detection of analytes in the highly sensitive region of the so-formed HS. To accomplish this objective, we have employed viologen dications (VGD). VGD posess several properties of interest to fulfill the above purposes; they are electron acceptors,[13,14] thus able to interact strongly with the metal surface, and they are able to form CT complexes with electron-donor species such as polycyclic aromatic hydrocarbons,[13] a group of pollutant compounds with a marked carcinogenous activity whose trace detection is nowadays of much importance.

In this work, we report the use of the VGD paraquat (PQ), diquat (DQ), and lucigenin (LG) (Figure 1) adsorbed on citrate Ag NPs as HS inductors and hosts for the detection of pyrene (PYR). Details on the preparation of citrate Ag NPs and on the UV−visible absorption spectra and Raman measurements were described in previous works.[15,16] The samples for SERS were prepared by first adding aqueous KCl until a final concentration of 3×10^{-2} M and then an aliquot of the viologen solution in water until the desired final VGD concentration. Finally, PYR (in acetone solution) was added to the viologen-functionalized Ag NPs until the desired final concentration. SERS measurements were performed in both macro- and microconditions.

The VGD were chosen in order to have a different structure with respect to the N atoms position and the extension of the aromatic part. Moreover, the VGD structure can modify the HS architecture, thus displaying specific physical and chemical tuning characteristics regarding the excitation wavelength and the pollutant with which they interact.

The Raman and SERS spectra of these VGD (Figure 1) display two bands in the 1550−1650 cm^{-1} region that are sensitive to the dication structure.[17] In general, the formation of CT complexes and the chemical reduction induce a weakening of the higher band above 1600 cm^{-1} and a strengthening of the band below this wavenumber. The Raman spectra of LG show similar profiles in the solid state (Figure 1a) and on Ag NPs (Figure 1b), with a weak band at 1627 cm^{-1}, indicating the high tendency of this dication to form CT complexes even in the absence of metal. In contrast, DQ exhibits a dramatic change in the Raman profile in going from the solid state (Figure 1c) to the adsorbed species on the metal surface (Figure 1d),

* To whom correspondence should be addressed. Fax: + 34 91 5 64 55 57. Phone: + 34 91 5 61 68 00. E-mail: imts158@iem.cfmac.csic.es.

10.1021/jp8006206 CCC: $40.75

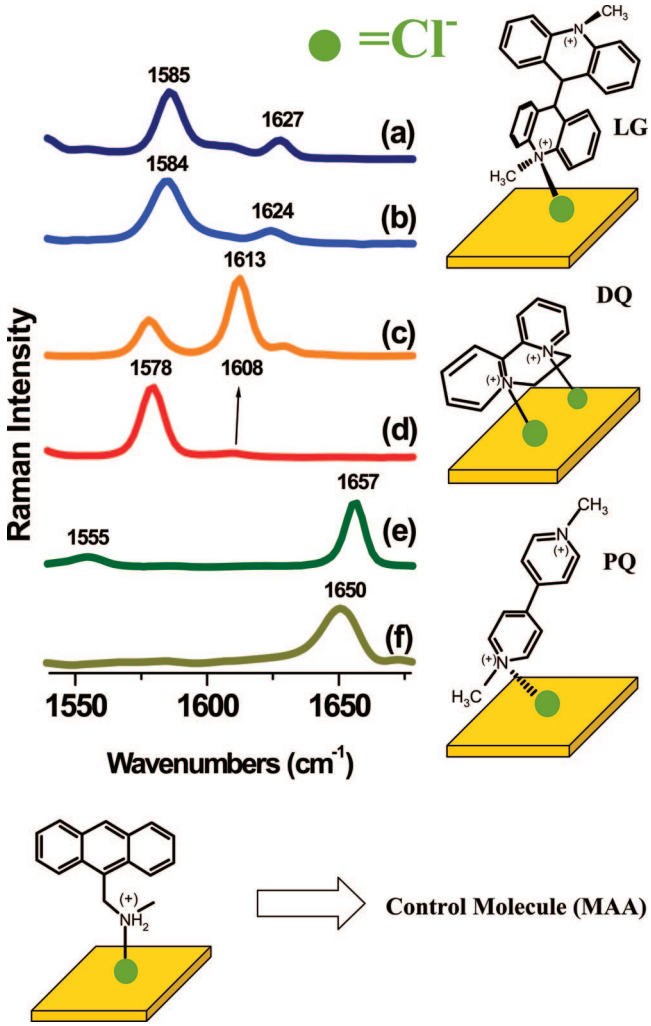

Figure 1. Top: Left panel: (a) Raman of LG in the solid state; (b) SERS spectrum of LG (10^{-6} M) on Ag NPs; (c) Raman of DQ in the solid state; (d) SERS spectrum of DQ (10^{-4} M) on Ag NPs; (e) Raman of PQ in the solid state; and (f) SERS spectrum of PQ (10^{-5} M). Right panel: Adsorption mechanism of LG, DQ, and PQ on the Ag surface showing the formation of a complex with the Cl^- anion adsorbed onto the Ag surface. Bottom: 9-(Methyl aminomethyl) anthracene (MAA), used as a control in SERS experiments. The excitation was set at 785 nm.

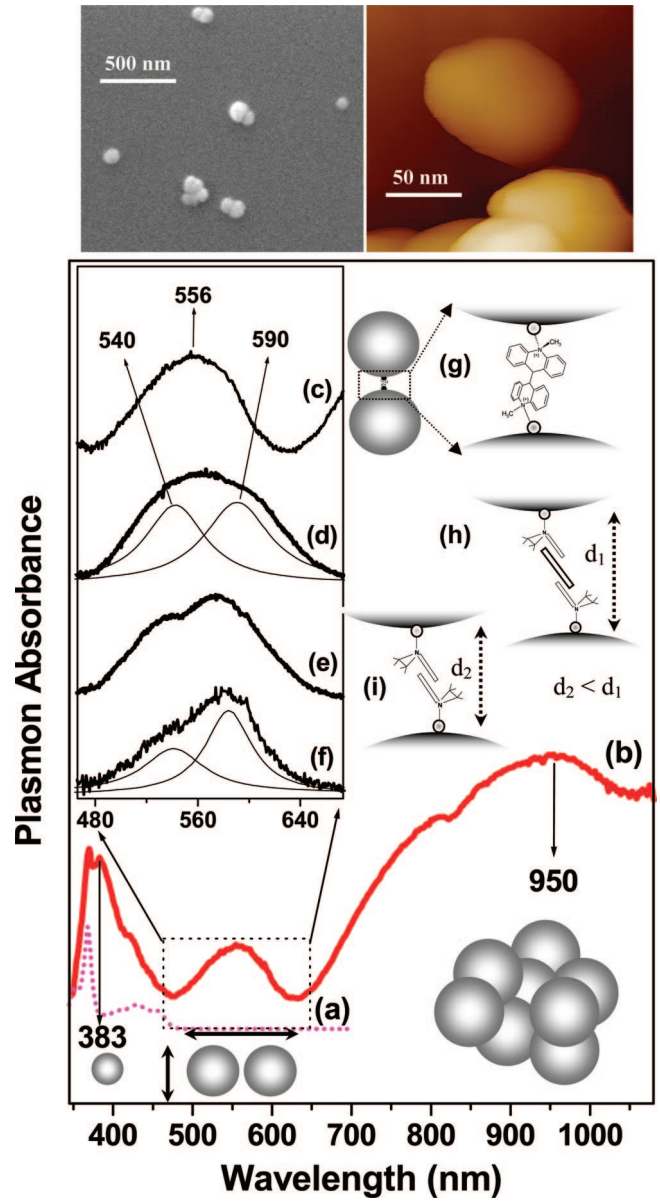

Figure 2. Top: SEM (left) and AFM (right) micrographs of Ag NPs showing the presence of dimers and interparticle junctions. Bottom: (a) Absorption spectrum of LG (10^{-4} M) in water; and (b) difference absorption spectrum of Ag NPs aggregated in the presence of LG (10^{-6} M), obtained upon subtraction of the absorption spectrum of Ag NPs aggregated with only chloride anions, displaying plasmon absorptions corresponding to monomer or transversal plasmons in chains (383 nm), longitudinal plasmons in dimers (500−600 nm), and multimers (broad band increasing above 700 nm). Inset: Detail of the plasmon absorbance band observed in the 500−600 nm region assigned to Ag NP dimers obtained upon aggregation with (c) LG (10^{-6} M); (d) DQ (10^{-4} M); (e) DQ (10^{-5} M); and (f) DQ (10^{-6} M). The first sample gave rise to a single band corresponding to the interparticle gap shown on the right (g). The three last spectra show two components assigned to the two different interparticle gaps induced by DQ shown on the right (h and i).

while PQ exhibits an intense band at 1657 cm^{-1} (Figure 1e) which does not change significantly when adsorbed on the metal (Figure 1f). These three different behaviors can be directly related to the structure of the above VGD regarding the position of the N atoms in the molecule and the extent of the aromaticity. The SERS spectra suggest that LG and DQ interact with the Ag surface through the formation of a CT complex with the adsorbed anion (chloride in this case), leading to a partial transition from sp^2 to sp^3 hybridation of the N atoms,[17] as indicated in the left panel schemes of Figure 1. In the case of PQ, this transition seems not to take place, most probably due to the weaker interaction with the Ag−Cl system and the probable formation of an ionic pair in this case. The interacting schemes presented for VGD (Figure 1, right panel) are in agreement with the data reported in the literature, where a perpendicular orientation was reported for LG on the metal surface.[18–20] Hence, LG is a good candidate to form junctions between NPs leading to HS.

The formation of HS after adding VGD was checked by the plasmon absorption of the Ag NPs suspension. Previously, the difference spectra between the absorption spectra of Ag NPs obtained in the presence of VGD and that recorded by adding only Cl^- anions were obtained in order to better see the contribution of VGD (Figure 2b). The UV−vis spectrum of LG (Figure 2a) was also added for comparison. In all cases, the difference spectra displayed three main bands appearing in the 370−390, 500−600, and 800−1000 nm regions, showing an increasing width toward longer wavelengths. The position of

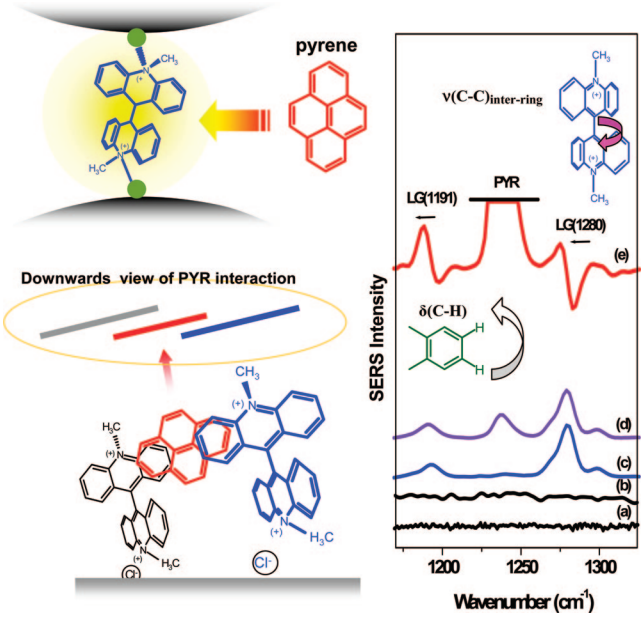

Figure 3. Right panel: SERS spectra of (a) PYR (10^{-5} M) on Ag NPs in the absence of a host molecule, (b) PYR (10^{-6} M) in MAA (10^{-5} M) after subtraction of the MAA SERS spectrum, (c) LG (10^{-6} M) and (d) LG (10^{-6} M) in the presence of PYR (10^{-6} M). (e) Difference between (d) and (c) spectra, showing the presence of a strong pyrene feature and shifts in key bands related to the LG structure. Left panel: Scheme of the detection strategy aimed at by using LG. Left panel: Top: Creation of a highly sensitive interparticle cavity induced by the adsorption of LG and approach of the pollutant PYR to the cavity. Bottom: Formation of intermolecular cavities necessary for the interaction with the electron donor. The excitation was set at 785 nm.

the first band practically did not change and can be assigned to nonaggregated Ag NPs or transversal plasmons in associated NPs chains. However, the position and width of the two latter bands remarkably changed depending on the structure and concentration of the adsorbed VGD. According to calculations carried out by Käll et al., the band appearing at 500−600 nm may correspond to the gaps between two Ag nanoparticles in dimers.[8] This is supported by the observation of dimers in these samples (Figure 2, top micrographs), while the band at the highest wavelength position may be due to larger aggregates or multimers, whose position is also dependent on the 500−600 nm band. The experimental evidence pointed out that large aggregates of NPs are the main source of the EM enhancement in colloids,[2] and although the formation of dimers seems to be a previous step in the appearance of these multimers, we suggest monitoring the effect of VGD on the architecture of NP suspensions by following the dimer plasmon band. The position of this band depends on the VGD structure (Figure 2c and d), but also on the concentration in the case of DQ (Figure 2d−f). In the latter case, both N atoms are directed to the same side, and thus, the presence of two or more dications is required to form interparticle junctions, whose distance can vary depending on the number of DQs placed between two Ag NPs (Figure 2h and i). In fact, two components are seen at 590 and 540 nm (Figure 2d−f), which can be attributed to junctions built by two or three DQs placed between Ag NPs (Figure 2h and i) on the basis of the distances predicted from the above configurations and the calculations reported by Käll et al.[8] The upper one increases as the concentration is lowered (Figure 2f) due to the higher electric field coupling existing when the interparticle distance is lower (Figure 2i).

No SERS signal from PYR was obtained either in the absence of VGD (Figure 3a, right panel) or upon functionalization of

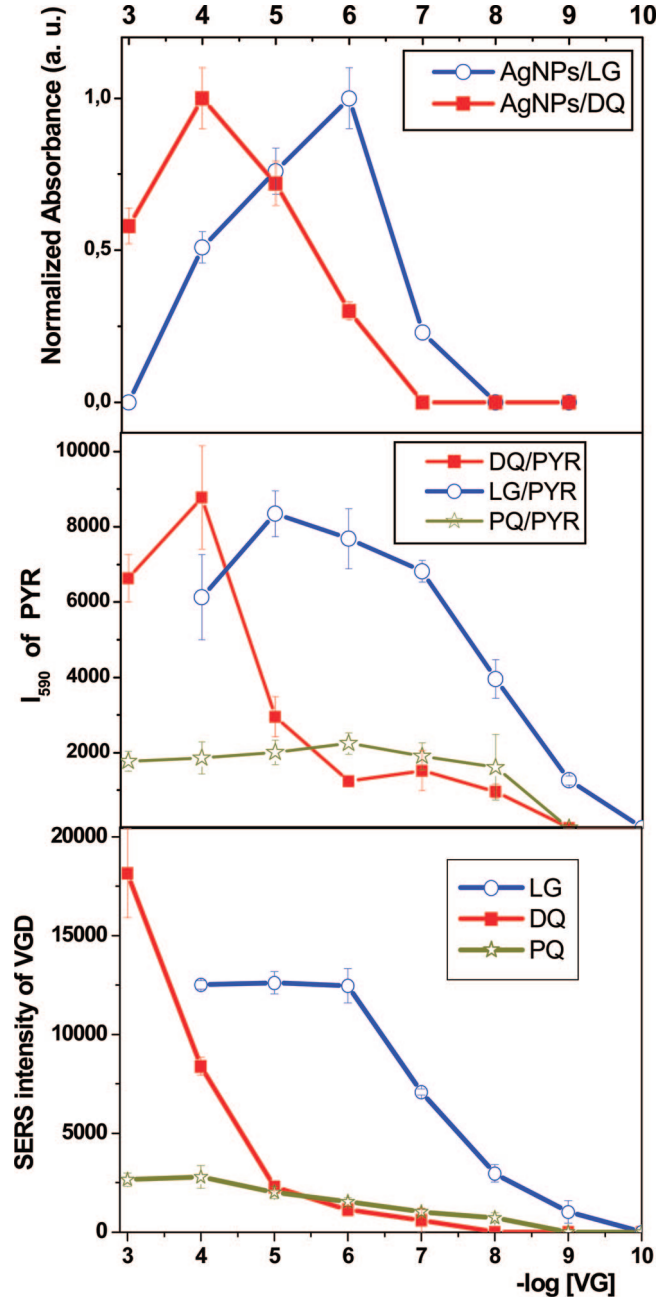

Figure 4. Top: Plasmon absorbance intensity of Ag NPs dimers in the 500−600 nm region against the VGD concentration. Middle: Intensity of the 590 cm^{-1} SERS characteristic band of PYR against the VGD concentration. Bottom: Intensity of the SERS spectra measured for the main band of VGD against the concentration of VGD.

the metal NPs by using 9-(methyl aminomethyl) anthracene (MAA, Figure 1), used here as an experimental control (Figure 3b). On the contrary, strong SERS signals from PYR could be obtained in the presence of LG on the metal surface (see the band at 1240 cm^{-1} in Figure 3d, right panel, and the difference spectrum of Figure 3e), which were not seen in the absence of VGD (Figure 3a). From this result, an effective interaction of PYR with LG was deduced (Figure 3, left panel). The LG−PYR interaction seems to take place through a CT complex which induces a rotation of the acridine rings, as deduced from the shift of the corresponding inter-ring C−C stretching band at 1280 cm^{-1}, and also of the aromatic C−H bending of the acridine moiety at 1191 cm^{-1} (Figure 3, right panel). The formation of intermolecular cavities between LG dications (Figure 3, left panel) due to the repulsion between the positive

charges existing in LG may be an important factor to allow the interaction of the pollutant with VGD and the formation of CT complexes as deduced from the inactivity of MMA, where these cavities seem not to be formed, in the detection of PYR.

The calculated enhancement factor for LG on AgNPs was approxiamtely 10.[8] This relatively high enhancement agrees with the formation of HS by LG. On the other hand, the importance of the HS building in the detection of PYR can be deduced from Figure 4. The intensity of the dimer plasmon absorbance in the 500−600 nm region (Figure 4, top panel) was plotted against the VGD concentration. As can be seen, LG reaches a maximum at 10^{-5} M in contrast to DQ, for which a maximum is seen at higher concentrations (10^{-4} M), most probably due to the need for a higher number of DQ dications to create HS interparticle junctions. Furthermore, this concentration dependence correlates very well with the SERS intensity variation seen at different VGD concentrations (Figure 4, bottom panel) and the SERS intensity variation observed for PYR (Figure 4, middle panel). The latter correlations clearly demonstrate the assignment of the above plasmon band to the interparticle junctions in dimers. Also, one can deduce that VGD are mainly placed in these junctions, where the pollutant molecules interacting with the host contribute to the main part of the overall pyrene SERS signal. The lower SERS effectiveness observed for PQ (Figure 4, middle and bottom panels) contrasts with the ability of this species to induce the formation of interparticle junctions, and this is presumably related to the different adsorption mechanism on metallic surfaces deduced for this dication reported elsewhere.[13] However, the overall intensification of both VGD and PYR SERS intensities could result from the combined effect of the existence of HS together with the enhancement effect provided by the effect of chloride ions also existing on the surface because of a charge-transfer mechanism, as reported previously.[21] The limit of detection (LOD) of PYR was measured by keeping the concentration of LG constant at 10^{-5} M and lowering the pollutant concentration. At these conditions, the lowest PYR concentration detectable was 10^{-9} M for LG. Further details on the SERS analysis of the VGD/PYR interaction deduced from the SERS spectra will be published in the near future for PYR in comparison to other PAHs.

In order to further demonstrate the importance of the Ag NPs aggregation directed by LG toward the fabrication of interparticle hot spots, we have carried out another control experiment consisting of the functionalization of an active Ag electrode (prepared as reported in ref 17) by LG. With this experiment, we expected to probe only the host ability of this VGD in the interaction with PYR. Thus, an acetone solution of PYR was exposed to the LG-functionalized electrode, showing no SERS signals corresponding to the pollutant.

In summary, we have demonstrated the efficiency of VG dications in the formation of highly sensitive HS localized in junctions between Ag NPs. The existence of these HS and their characteristics can be followed by the plasmon absorption attributed to the dimers appearing in the 500−600 nm region. The interest in these VGD species is double: as builders of sensitive areas of giant electromagnetic field enhancement and as hosts to selectively interact with pollutants, taking advantage of the formation of intermolecular cavities. The selectivity properties displayed by VGD regarding other PAHs and chlorinated pesticides will be analyzed in a future work. Furthermore, the ability of certain molecules to create highly sensitive HS accounts for the extraordinary SERS intensification detected in the case of other very well-known molecular species such as rhodamine and crystal violet dyes. In fact, these compounds are usually employed in SMD because of the creation of a high amount of HS due to their bifunctionality, where they are mainly placed, and their huge Raman resonance intensification.[22]

Acknowledgment. We acknowledge project FIS2007-63065 from Dirección General de Investigación, Ministerio de Educación y Ciencia and Comunidad Autonoma de Madrid Project Number S-0505/TIC/0191 MICROSERES for financial support. L.G. acknowledges an I3P fellowship from CSIC.

References and Notes

(1) Moskovits, M. *Rev. Mod. Phys.* **1985**, *57*, 783.
(2) Aroca, R. *Surface-Enhanced Vibrational Spectroscopy*; John Wiley & Sons: Chichester, U.K., 2006.
(3) Nie, S.; Emory, S. R. *Science* **1997**, *275*, 1102.
(4) Kneipp, K.; Wang, Y.; Kneipp, H.; Perelman, L. T.; Itzkan, I.; Dasari, R. R.; Feld, M. S. *Phys. Rev. Lett.* **1997**, *78*, 1667.
(5) Otto, A. *J. Raman Spectrosc.* **2006**, *37*, 937.
(6) Futamata, M. *Faraday Discuss.* **2006**, *132*, 45.
(7) Le Ru, E. C.; Etchegoin, P. G.; Meyer, M. *J. Chem. Phys.* **2006**, *125*, 204701.
(8) Käll, M.; Xu, H.; Johansson, P. *J. Raman Spectrosc.* **2006**, *36*, 510.
(9) Olk, P.; Renger, J.; Härtling, T.; Wenzel, M. T.; Eng, L. M. *Nano Lett.* **2007**, *7*, 1736.
(10) Anderson, D. J.; Moskovits, M. *J. Phys. Chem.* **2006**, *110*, 13722.
(11) Lee, S. J.; Morrill, A. R.; Moskovits, M. *J. Am. Chem. Soc.* **2006**, *128*, 2200.
(12) Aroca, R. F.; Alvarez-Puebla, R.; Pieczonka, N.; Sanchez-Cortes, S.; Garcia-Ramos, J. V. *Adv. Colloid Interface Sci.* **2005**, *116*, 45.
(13) Monk, P. M. S. *The Viologens: Physicochemical Properties, Synthesis and Applications of the Salts of 4,4′-Bipyridine*; John Wiley and Sons: Chichester, U.K., 1998.
(14) Monk, P. M. S.; Hodgkinson, N. M. *Electrochim. Acta* **1998**, *43*, 245.
(15) Cañamares, M. V.; García Ramos, J. V.; Gómez-Varga, J. D.; Domingo, C.; Sanchez-Cortes, S. *Langmuir* **2005**, *21*, 8546.
(16) Guerrini, L.; García-Ramos, J. V.; Domingo, C.; Sanchez-Cortes, S. *Langmuir* **2006**, *22*, 10924.
(17) Millán, J. I.; Sanchez-Cortes, S.; García-Ramos, J. V. *J. Electroanal. Chem. A* **2003**, *107*, 9611.
(18) Tang, X. Y.; Schneider, T.; Buttry, D. A. *Langmuir* **1994**, *10*, 2235.
(19) Lopez-Ramirez, M. R.; Guerrini, L.; Garcia-Ramos, J. V.; Sanchez-Cortes, S. *Vib. Spectrosc.* Accepted; doi:10.1016/j.vibspec.2007.12.003.
(20) Millán, J. I.; Sanchez-Cortes, S.; García-Ramos, J. V.; Rodríguez-Amaro, R. *J. Raman Spectrosc.* **2003**, *34*, 227.
(21) Otto, A.; Bruckbauer, A.; Chen, Y. X. *J. Mol. Struct.* **2003**, *661−662*, 501.
(22) Michaelis, A. M.; Jiang, J.; Brus, L. *J. Phys. Chem. B* **2000**, *104*, 11965.

JP8006206